This article has been accepted for publication in a future issue of this journal, but has not been fully edited. Content may change prior to final publication. Citation information: DOI 10.1109/TBME.2018.2885781, IEEE Transactions on Biomedical Engineering

Correlation Between Optical Fluorescence and Microwave Transmission During Single-cell Electroporation

Hang Li, Xiao Ma, *Student Member, IEEE,* Xiaotian Du, *Student Member, IEEE,* Lei Li, *Student Member, IEEE,* Xuanhong Cheng*, and James C. M. Hwang, *Life Fellow, IEEE*

***Abstract*— *Objective:* Multimodal characterization of a mammalian cell by optical and microwave techniques simultaneously during electroporation. *Methods:* Using a coplanar waveguide with a Jurkat cell trapped in the middle of its center conductor, continuous waves at 100 kHz of different amplitudes were applied for 20 s while microwave transmission coefficients at 9 GHz were measured every 0.4 s. *Results:* The onset of electroporation was indicated by abrupt changes in both fluorescence intensity and transmission coefficient. Additionally, in measurements that lasted 300 s, the transmission coefficient was found to recover to the pre-poration level, while the fluorescence intensity remained different. Since the cells were confirmed viable through post-poration staining, the recovery of the transmission coefficient suggested reversible electroporation. *Conclusion:* These experimental results showed that the transmission coefficient could serve as a label-free indicator of cell membrane permeability during and after electroporation. Furthermore, it could be used to expeditiously differentiate reversible electroporation from the irreversible one. *Significance:* This study should aid fundamental analysis of cell physiology, as well as molecular delivery in cell engineering and electrotherapy.**

***Index Terms*— Biosensors, electroporation, cellular biophysics, microwave measurement, impedance spectroscopy.**

I. Introduction

ELECTROPORATION is a widely used physical (as opposed to chemical or biological) method to enhance the permeability of a cell membrane, with the degree of enhancement determined by applied field magnitude, duration, frequency, etc. [1]. *Reversible* electroporation has been used to transfect a cell or to deliver molecules into a cell for both fundamental research and clinical treatment, thereafter the membrane heals gradually and the cell remains viable. On the other hand, *irreversible* electroporation creates a permanent damage to the membrane that leads to cell death and has gained interest in tumor ablation. Strictly speaking, in response to the applied field, nanopores may form and heal in nanoseconds, which is followed by a period of enhanced permeability that can last for seconds. In this paper, we do not attempt to differentiate electroporation from electro-permeabilization.

Traditional electroporation is based on a kilovolt pulse generator which applies a high voltage across two parallel-plate electrodes with a spacing on the order of 1 mm, within which a large number of cells are suspended in a conductive medium. This makes the setup not only bulky and costly, but also dangerous. The high voltage can also cause side effects such as heating, electrolysis, and generation of other reactive chemicals. Most importantly, despite the high voltage, the poration efficiency rarely exceeds 50%, so that the fundamental dynamics for poration and healing of individual cells are buried in an ensemble of both porated and unporated cells.

By contrast, *single-cell* electroporation based on a microfluidic setup allows directly observation of poration and healing dynamics of individual cells [2]. The applied voltage can be reduced to the order of 1 V, the same as the transmembrane potential. The low voltage can be fine-tuned to increase poration efficiency without compromising cell viability, as well as to slow down the cell response so that the poration and healing dynamics can be monitored in real time by fluorescence microscopy.

Traditionally, electroporation is characterized optically. For example, cell poration can be indicated by the red fluorescence of propidium iodide (PI) [3], whereas cell viability can be indicated by the green fluorescence of calcein acetoxymethyl (calcein AM) [4]. Before poration, the intact membrane prevents PI from entering a cell. Once porated, PI diffuses into the cell to bind with DNA, resulting in red fluorescence of the nucleus. In a viable cell, the nonfluorescent calcein AM is converted to green-fluorescent calcein. Once the cell membrane is permanently compromised, most of the calcein AM diffuses out so that the green fluorescence diminishes. Other than fluorescence microscopy, bright-field microscopy of cell swelling due to osmotic imbalance has also been proposed as a poration indicator [5]. As all these optical characterization

Manuscript received February 21, 2018; revised August 31 and October 28, 2018. This work was supported in part by the U.S. Department of Defense, Defense Threat Reduction Agency under Grant HDTRA1-12-1-0007, Army Research Office under Grant W911NF-14-1-0665, and Air Force Office of Scientific Research under Grant FA9550-16-1-0475 as well as National Science Foundation under Grant ECCS-1809623. This work was performed in part at the Cornell NanoScale Facility, a member of the National Nanotechnology Coordinated Infrastructure, which is supported by the U.S. National Science Foundation under Grant ECCS-1542081. Asterisk indicates corresponding author.

H. Li and X. Cheng* are with Bioengineering as well as Materials Science and Engineering, Lehigh University, Bethlehem, PA 18015, USA (correspondence e-mail: xuc207@lehigh.edu).

X. Ma, X. Du, Lei. Li and J. C. M. Hwang are with Electrical and Computer Engineering, Lehigh University, Bethlehem, PA 18015, USA.

0018-9294 (c) 2018 IEEE. Personal use is permitted, but republication/redistribution requires IEEE permission. See http://www.ieee.org/publications_standards/publications/rights/index.html for more information.

This article has been accepted for publication in a future issue of this journal, but has not been fully edited. Content may change prior to final publication. Citation information: DOI 10.1109/TBME.2018.2885781, IEEE Transactions on Biomedical Engineering

techniques rely on diffusion of dyes or solutes, their response can be slow.

Traditionally, electrical impedance measurement has also been used to monitor the change at kilohertz frequencies of the membrane impedance due to poration, and the change at megahertz frequencies of the cytoplasm impedance due to ion diffusion [6]. Compared to optical characterization, electrical characterization can be fast and label-free. However, at these low frequencies, the impedance measurement can be masked by ion current and the double layer formed between an electrode and an electrolyte. As the result, impedance measurements have been better correlated with the cytoplasm change *after* poration than the membrane change *during* poration [7]. Additionally, for most single-cell electroporation setups, uniform field assumption and Maxwell-Wagner mixture model are no longer valid.

To avoid the complication of ion current and double layer at low frequencies, electrical characterization was recently performed at 5 GHz on single cells to assess their viability 24 h *after* electroporation and validated by trypan blue staining [8]. However, electroporation and staining were performed on cell suspensions separately, and the percentage of viable cells was affected by those that multiplied during the 24-h incubation period.

So far, little is known about the changes of the cell electrical property during the poration process. Optical monitoring, although widely used, can be unreliable in revealing the reversibility of poration. To overcome these limitations, we have used a uniquely linear and ultrawideband setup in conjunction with a continuous-wave (CW) sinusoidal signal on the order of 1 V to characterize single cells in real time *during* poration, both optically and electrically [9]. The measured microwave transmission coefficient at 9 GHz was found to correlate with cell swelling by electroporation. This paper expands on [9] by adding PI and calcein-AM fluorescence microscopy to bright-field microscopy and microwave characterization, all in real time both *during* and *after* electroporation. This way, for the first time, the microwave transmission coefficient was validated as a label-free indicator of both cell poration and cell viability, so that reversible and irreversible electroporation could be electrically distinguished at the single-cell level. The details will be described in the following, according to a standard order of setup, result, discussion, and conclusion.

II. Experimental Setup and Test Protocol

The experimental set up comprised a home-made microwave probe station on a Nikon Eclipse TE2000 inverted fluorescence microscope as described in [9], except detailed electrode design as shown in Fig. 1. The test chip comprised a gold coplanar waveguide (CPW) intersected by a polydimethylsiloxane (PDMS) cover at a right angle. The length, width, and thickness of the PDMS cover were 8 mm, 5 mm, and 4 mm, respectively. The bottom side of the PDMS cover was etched with a microfluidic channel 5-mm long, 200-µm wide, and 20-µm deep. The CPW was fabricated in 0.5-µm-thick gold on 500-µm-thick quartz. The CPW was 1-cm long and its center

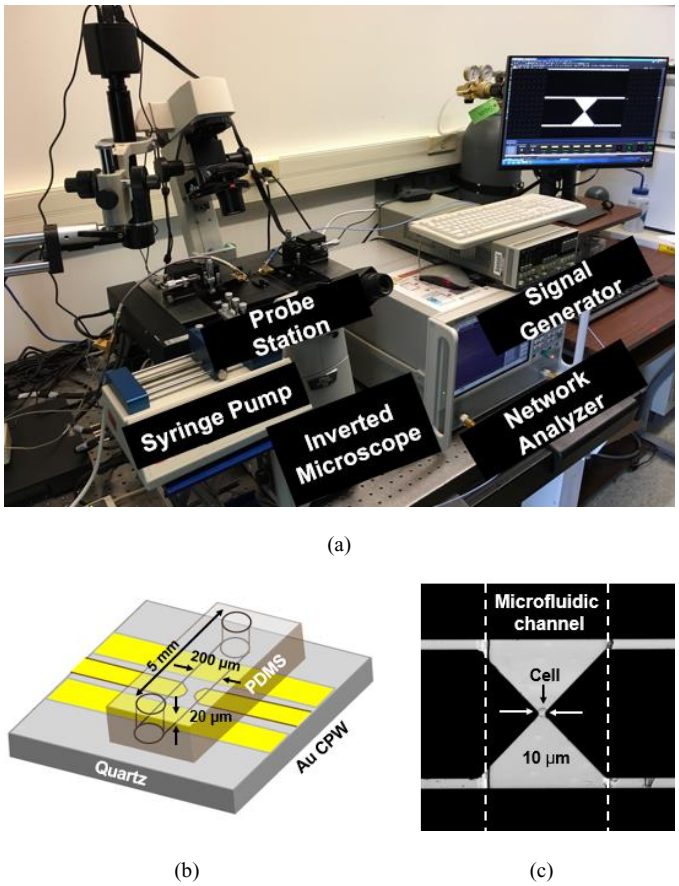

Fig. 1. (a) Photograph of the experimental set up, and (b) schematic and (c) micrograph of the test chip. In (c) a Jurkat cell was trapped between two tapered sections of the center electrode of a coplanar waveguide, which were 10-µm apart.

electrode was mostly 200-µm wide except under the microfluidic channel, where it was tapered down to 10 µm with a 10-µm gap in the middle. The spacing between the center electrode and the ground electrodes of the CPW was 16 µm except in the tapered region. The CPW was designed with a 50-Ω characteristic impedance across an ultrawideband of 9 kHz to 9 GHz before the tapers.

Alternating-current dielectrophoresis (AC DEP) was used to trap a single cell at the gap in the middle of the CPW center electrode. A DEP signal of 5 MHz, 2.2 V (4.4 V peak-to-peak) was supplied by a Hewlett Packard 8116A pulse/function generator and coupled via a bias tee to the CPW input. With the DEP signal on, cell suspension was flowed through the microfluidic channel until a cell was trapped, which usually took a few seconds as confirmed through the microscope. Once a cell was trapped, the DEP signal was turned off, the flow was paused to avoid dislodging the trapped cell, and the pulse/function generator was switched to a poration signal of 100-kHz CW with different amplitudes up to 2.5 V. Meanwhile, the magnitude of the microwave transmission coefficient $|S_{21}|$ was measured on the CPW output at 9 GHz in 0.4-s intervals by a Keysight Technologies E5080A network analyzer with an input power of −18 dBm to minimize heating or any other side effects [10]. For each poration voltage, three separate experiments were conducted on three different cells to ensure

0018-9294 (c) 2018 IEEE. Personal use is permitted, but republication/redistribution requires IEEE permission. See http://www.ieee.org/publications_standards/publications/rights/index.html for more information.

This article has been accepted for publication in a future issue of this journal, but has not been fully edited. Content may change prior to final publication. Citation information: DOI 10.1109/TBME.2018.2885781, IEEE Transactions on Biomedical Engineering

the result was statistically meaningful. In all cases, the poration signal was applied for 20 s, whereas the transmission coefficient was measured up to 300 s.

Usually,

$$|S_{21}| = \sqrt{P_T / P_I} \le 1, \tag{1}$$

where P_I and P_T are the powers of incident and transmitted waves, respectively. Therefore, $\log|S_{21}| < 0$. Dividing the transmission coefficient measured after cell trapping with that measured just before cell trapping, the small difference due to trapping and poration of a single cell could be reliably obtained. In terms of decibel (dB),

$$\begin{aligned} 10\cdot\log|\Delta S_{21}| &= 10\cdot\log\left|S_{21}(\text{w/ cell})/S_{21}(\text{w/o cell})\right| \\ &= 10\cdot\log\left|S_{21}(\text{w/ cell})\right| - 10\cdot\log\left|S_{21}(\text{w/o cell})\right| \end{aligned}. \tag{2}$$

Thus, a negative $\log|\Delta S_{21}|$ implies that $|S_{21}(\text{w/ cell})| < |S_{21}(\text{w/o cell})|$ and the presence of a cell decreases microwave transmission. This can be explained by considering that at 9 GHz, microwave transmission across a cell is mainly determined by cytoplasm instead of membrane properties [11]. Since the dielectric constant of the cytoplasm is lower than that of the sucrose solution [10], $\log|\Delta S_{21}|$ is negative initially, and, once the cell is porated, it becomes less negative as the cell equilibrates with the sucrose solution.

To correlate with the microwave measurements, morphology and fluorescence intensity of the same cell were simultaneously recorded by a high-speed three-color video camera through the microscope. As in [10], 2 μM of PI dye was used to confirm cell poration, whereas 2 μM of calcein AM was used to confirm cell viability. Following [12], we defined cell poration as when the red fluorescence intensity increased by 5% from its initial value, and cell death as when the green fluorescence intensity decreased by more than 40% of its peak value. The red and green fluorescence images, along with a bright-field image, of the same cell were recorded by the video camera every second in real time. From the acquired images, overall fluorescence intensity and cell size were calculated by integration over the entire cell using the ImageJ software.

For proof of concept, Jurkat T lymphocyte human cells were used given their relatively simple structure and nonadherent nature. As reported previously [10], [11], Jurkat cells were cultured in an RPMI 1640 medium. Before flowing through the microfluidic channel, Jurkat cells were centrifuged three times at 750 rpm for 5 min, and resuspended in an isotonic solution with 8.5% sucrose and 0.3% dextrose at a concentration of 3×10^6 cell/mℓ. The solution was supplemented with 2 μM of PI and 2 μM of calcein AM. Cells were incubated in dark for 1 h before flowing through the microfluidic channel at 0.1 μℓ/min as controlled by a syringe pump. In separate experiments involving a Coulter counter and trypan blue dye (0.4 wt. %), cells were confirmed to have a diameter of 9.9 ± 1.3 μm and a survival rate of > 50% after 10 h [10], [11].

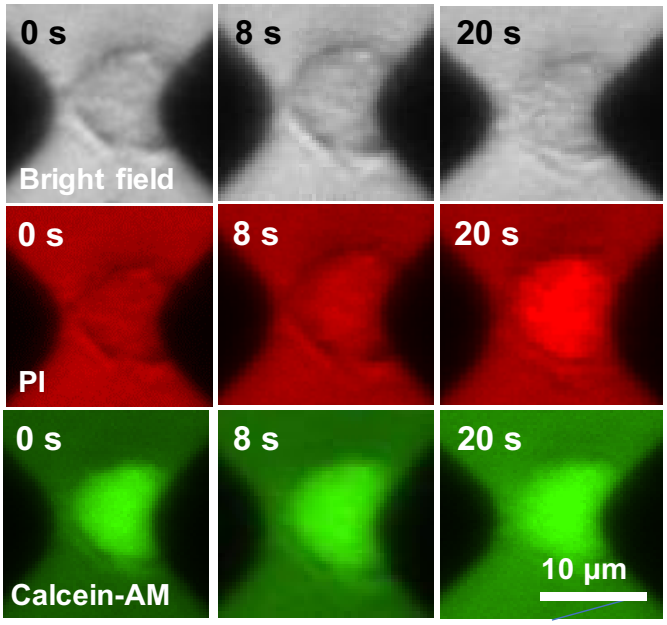

(a)

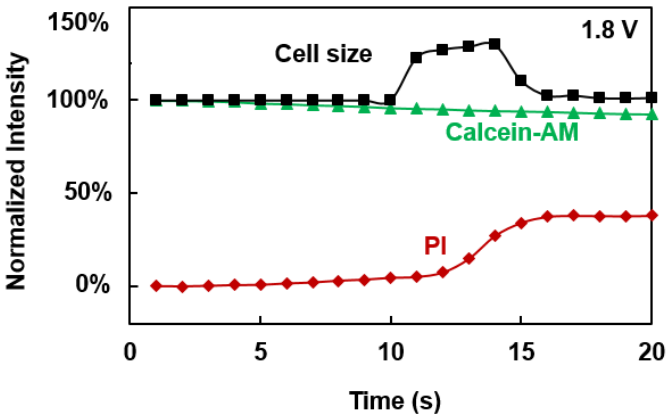

(b)

Fig. 2. Optical characterization of the morphology, poration, and vitality of a Jurkat cell *during* exposure to a poration signal of 100 kHz and 1.8 V. (a) Representative bright-field (top row), red-fluorescence (PI, middle row), and green-fluorescence (Calcein-AM, bottom row) images taken after 0, 8, and 20 s of exposure. (b) Evolution of normalized cell size (■), red fluorescence intensity (♦), and green fluorescence intensity (▲).

III. Experimental Results

Using the above-described experimental setup and test protocol, we first confirmed in real time by optical microscopy that the 100-kHz CW signal was effective in inducing poration on a Jurkat cell in approximately 10 s, provided the amplitude of the poration signal was 1.5 V or higher. Further, poration coincided with cell swelling without significant change in cell vitality. Fig. 2(a) shows sample images of cell morphology and red/green fluorescence before, during, and after 20 s exposure to a 100-kHz, 1.8-V poration signal. It can be seen that after 8 s of exposure, the red fluorescence starts to appear at the top left corner of the cell, and it diffuses through the whole cell after 17 s, indicating effective poration. Based on the images of Fig.

0018-9294 (c) 2018 IEEE. Personal use is permitted, but republication/redistribution requires IEEE permission. See http://www.ieee.org/publications_standards/publications/rights/index.html for more information.

This article has been accepted for publication in a future issue of this journal, but has not been fully edited. Content may change prior to final publication. Citation information: DOI 10.1109/TBME.2018.2885781, IEEE Transactions on Biomedical Engineering

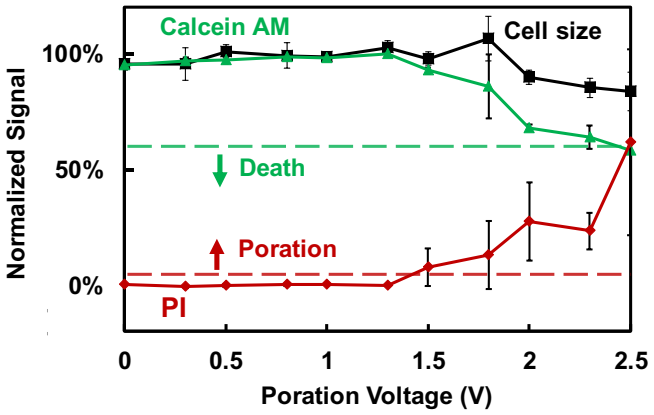

Fig. 3. Normalized cell size (■), red fluorescence intensity (♦), and green fluorescence intensity (▲) of a Jurkat cells *after* 20-s exposure to 100-kHz poration signals with different amplitudes. Error bars indicate standard deviation between three different cells subjected to the same exposure.

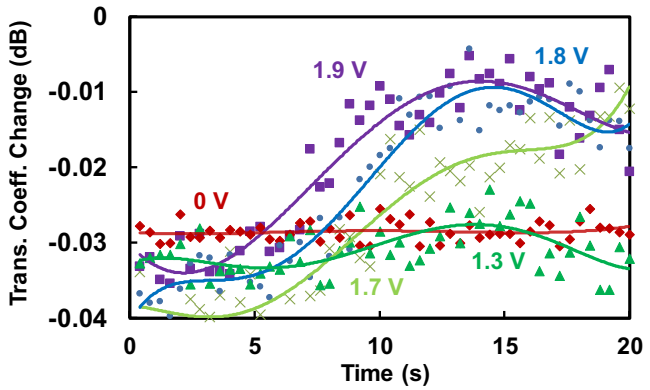

Fig. 4. Typical timecourse of the transmission coefficient change measured at 9 GHz from single Jurkat cells *during* exposure to a 100-kHz poration signal with amplitudes of 0 V (♦), 1.3 V (▲), 1.7 V (x), 1.8 V (●), and 1.9 V (■). Solid curves are polynomial least-square fits to guide the eyes.

2(a), Fig. 2(b) plots the evolution of cell size, poration, and vitality, respectively. It can be seen that after 8 s of exposure, the red fluorescence intensity increases by approximately 5%, which agrees with the criterion for poration. Meanwhile, the green fluorescence intensity decreases steadily, and, in 20 s, it decreases by approximately 10%, which is less than the 40% criterion for cell death. In this case, the cell is considered viable post-poration. Fig. 2(b) shows also that after 10 s exposure, the cell swells by approximately 25% and the swelling lasts only approximately 5 s, suggesting that as poration proceeds the pore size increases so that by then even large molecules can permeate through the cell membrane to reestablish osmotic equilibrium [5], [13].

The optical characterization suggests that a window between 1.5 V and 2.0 V exists for *reversible* poration. To determine the poration threshold voltage, the amplitude of the 100-kHz poration signal was varied from 0 to 2.5 V with the cell response characterized optically. Following the above- described image analysis, Fig. 3 plots the changes of cell size and fluorescence intensity after 20 s exposure to different voltages. It can be seen that below 1.5 V, both fluorescence intensities are steady and the cell-to-cell variability is small, leading to invisible error bars. From the red fluorescence intensity, it is observed that two cells are porated at 1.5 V whereas the other cell is not, indicating 1.5 V as the poration threshold (red dash line on Fig. 3). At 2.0 V, all three cells are porated, but one cell also starts to die as indicated by a significant drop of green fluorescence intensity. At 2.5 V, all three cells are dead after 20-s exposure.

Also observed through optical characterization, the trend for the change of cell size was similar to that of the fluorescence intensity. On average, the cell size *post* poration remains relatively constant below 1.8 V, above which shrinkage increases with increasing voltage. This shrinkage *after* poration is different from the temporary swelling *during* poration as illustrated in Fig. 2(b). Despite the interesting observation of cell swelling and shrinkage, since the onset of swelling has already been correlated with the shift in microwave transmission coefficient [9], in this paper we focus on correlating fluorescence microscopy with microwave characterization. It suffices to say that since the microwave transmission coefficient does not exhibit a correspondingly temporary "swelling" or "shrinkage," its shift is not purely a size effect.

Most significantly in this study, the microwave transmission coefficient was found to correlate with the fluorescence intensity *during* electroporation. Fig. 4 illustrates typical changes of the transmission coefficient upon exposure to 100-kHz poration signals of 0, 1.3 V, 1.7 V, 1.8 V and 1.9 V. The first two amplitudes are below the threshold, while the last three are above the threshold, but within the range of reversible poration. Despite the scattered data in each case, it can be seen that the transmission coefficient is rather flat at 0 V and 1.3 V, but shifts upward significantly at 1.7 V, 1.8 V, and 1.9 V. Further, the higher the amplitude, the sooner the shift. This shift can be explained by porated cells equilibrating with the surrounding sucrose solution as discussed in the previous section. This shows that the transmission coefficient can be used as a label-free poration indicator. Within the reversible poration range, the change of ΔS_{21} does not seem to have an obvious dependence on the poration signal amplitude.

The poration signal amplitude was further increased to the irreversible range as shown in Fig. 5. Fig. 5(a) plots the net shift of the transmission coefficient *after* 20-s exposure to a 100-kHz poration signal with different amplitudes. It can be seen that the transmission coefficient shifts significantly at 1.5 V or above, which is consistent with that of the fluorescence intensity shown in Fig. 3. Consistent also with the fluorescence intensity, the transmission coefficient exhibits a significantly larger error bar above 1.5 V, indicating different poration susceptibilities of different cells. The consistent transmission coefficient below 1.3 V also suggests that the cells are stably positioned during poration as confirmed through the microscope. However, Fig. 5(b) shows that even before the transmission coefficient and the error bar increases significantly at 1.5 V, the transmission coefficient becomes significantly more scattered above 0.5 V, which can also be seen from the 1.3-V data in Fig. 4. Presently, the mechanism and significance of such sub-threshold increase in the scatter of the transmission coefficient are unclear. The error bars in Fig. 5(b) represent standard deviations among

0018-9294 (c) 2018 IEEE. Personal use is permitted, but republication/redistribution requires IEEE permission. See http://www.ieee.org/publications_standards/publications/rights/index.html for more information.

This article has been accepted for publication in a future issue of this journal, but has not been fully edited. Content may change prior to final publication. Citation information: DOI 10.1109/TBME.2018.2885781, IEEE Transactions on Biomedical Engineering

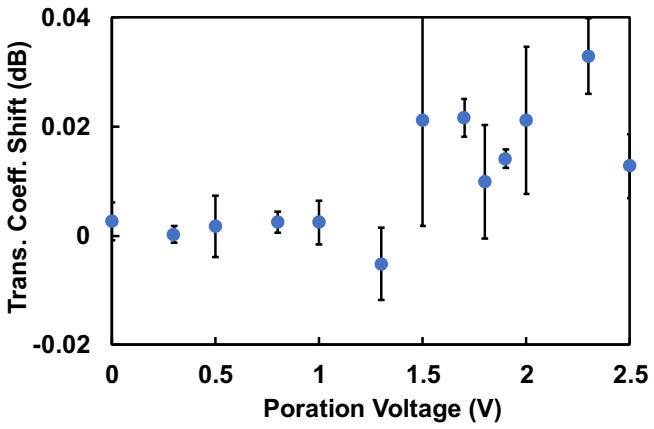

(a)

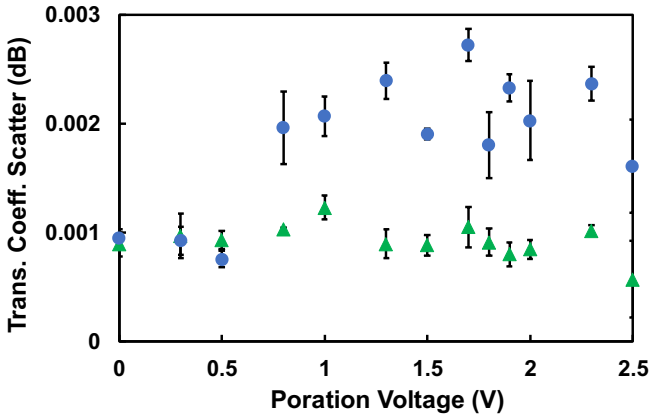

(b)

Fig. 5. (a) Net shift and (b) scatter in the transmission coefficient measured at 9 GHz with (●) and without (▲) a Jurkat cell *after* 20-s exposure to a 100-kHz poration signal with different amplitudes. Error bars indicate standard deviation among three different cells subjected to the same exposure in three different experiments.

three different cells at each voltage. The standard deviation is obtained from the time-dependent change in the transmission coefficient of Fig. 4. First, the moving average of every five data points is calculated. Next, the error between the data and the moving average is calculated at each voltage. Finally, the standard deviation is calculated from the errors of three cells at each voltage.

Both the fluorescence intensity and the transmission coefficient could be used to distinguish reversible electroporation from irreversible electroporation. Optically, after exposure to 1.5–2.0 V for 20 s, some cells appeared to uptake PI by more than 5% but lost less than 40% calcein AM, suggesting they might have been reversibly porated. To confirm that they were indeed viable long after poration, selected cells were continuously monitored up to 280 s after the poration signal was turned off. Fig. 6 illustrates the response of a cell exposed to a 100-kHz, 1.6-V poration signal. It can be seen that after the 20-s exposure, the red fluorescence intensity increases by 26%, the green fluorescence intensity decreases by 19%, and the transmission coefficient increases by 0.01 dB. With the poration signal off, the fluorescence intensities remain constant

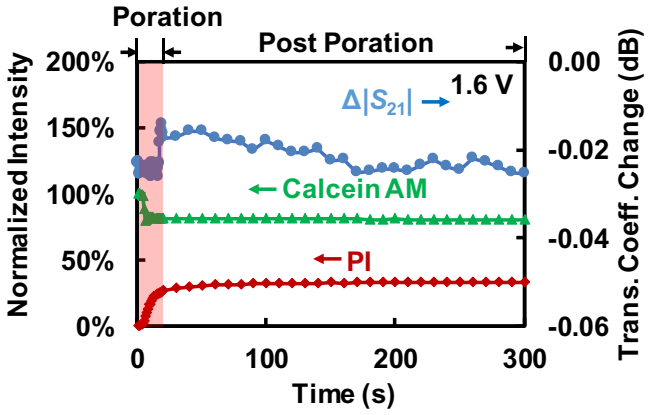

(a)

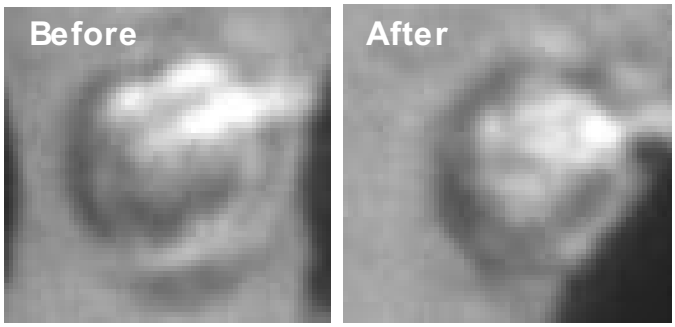

(b)

Fig. 6. Simultaneus optical and microwave characterization of a Jurkat cell during and *after reversible* poration with a 100-kHz, 1.6-V signal for 20 s. (a) Evolution of changes in red fluorescence intensity (♦), green fluorescence intensity (▲), and microwave transmission coefficient (●). (b) Bright-field images before and after trypan blue staining approximately 20 min after poration.

but the transmission coefficient gradually recovers to its initial value at approximately 180 s and remains constant thereafter.

In addition to being a poration indicator, the microwave transmission coefficient can be a label-free indicator of cell healing after reversible poration. Since presently there is no convenient way to collect a porated cell for clonogenic assay, to confirm that a cell remained viable long after poration, the same porated cell was stained *in situ* with trypan blue 20 min after poration and found to exhibit no change in the optical density [Fig. 6(b)]. This indicated that the cell membrane healed and the cell was viable at this point. To stain the cell with trypan blue, the flow was resumed but switched from a sucrose solution supplemented with PI and calcein AM to another one supplemented with trypan blue. With the flow rate kept low to avoid dislodging the cell, it took approximately 20 min for trypan blue to reach the cell.

The correlation between reversible electroporation and recoverable microwave transmission coefficient was further confirmed by analyzing the recovery of the transmission coefficient up to 280 s after a cell was porated with a 100-kHz signal of 1.7 V or 1.9 V for 20 s. It can be seen in Fig. 7 that at 1.7 V, the transmission coefficient fully recovers after approximately 110 s similar to the 1.6-V case shown in Fig. 6. At 1.9 V, the transmission coefficient recovers at a slower rate

0018-9294 (c) 2018 IEEE. Personal use is permitted, but republication/redistribution requires IEEE permission. See http://www.ieee.org/publications_standards/publications/rights/index.html for more information.

This article has been accepted for publication in a future issue of this journal, but has not been fully edited. Content may change prior to final publication. Citation information: DOI 10.1109/TBME.2018.2885781, IEEE Transactions on Biomedical Engineering

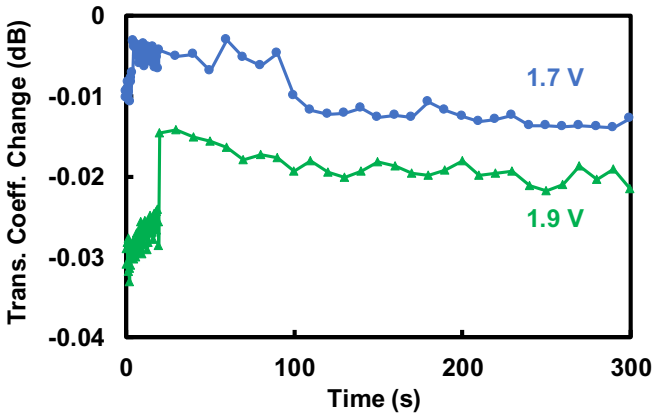

Fig. 7. Recovery of the microwave transmission coefficient after a Jurkat cell was *reversibly* porated by a 100-kHz signal of 1.7 V (●) or 1.9 V (▲) for 20 s.

so that the recovery is incomplete after 300 s. This indicates that although the cell is not dead as in the 2.0-V case (Fig. 8), it suffers greater disturbance than the cases at lower voltages and, hence, takes longer to heal.

Thus, the microwave transmission coefficient can be used to indicate *irreversible* poration, too. In contrast to reversible electroporation, Fig. 8 shows the response of a cell exposed to 100 kHz, 2.0 V for 20 s, which was previously determined by optical characterization to be the threshold to induce cell death. It can be seen from Fig. 8(a) that after poration, the transmission coefficient not only shifts significantly, but also never recovers to its initial value even after 300 s. Fig. 8(b) confirms that approximately 20 min after poration, the bright-field image with trypan blue is significantly darker than the one without trypan blue, indicating cell death.

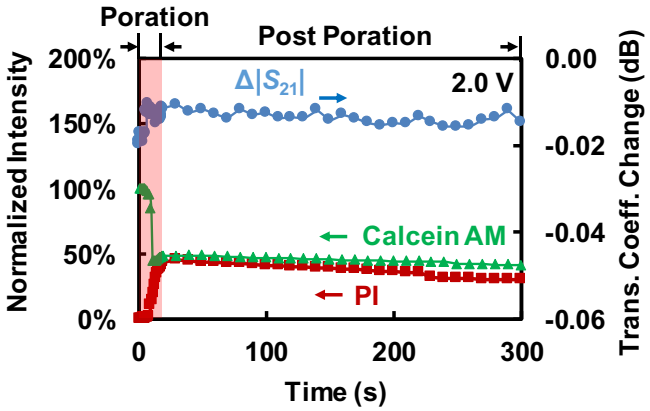

(a)

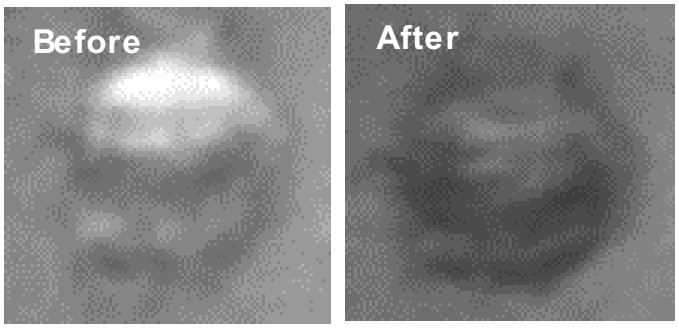

(b)

Fig. 8. Simultaneus optical and microwave characterization of a Jurkat cell during and *after irreversible* poration with a 100-kHz, 2.0-V signal for 20 s. (a) Evolution of changes in red fluorescence intensity (♦), green fluorescence intensity (▲), and microwave transmission coefficient (●). (b) Bright-field images before and after trypan blue staining approximately 20 min after poration.

IV. Discussion

Different from most other electroporation setups, we apply the electrical field in CW instead of pulses. The AC field reduces electrolysis and generation of other reactive chemicals. It has been shown that electroporation based on an AC field has superior performance than conventional pulse electroporation due to less polarization and sonication effect [14], [15]. In another study, electroporation with bipolar square waves was found to result in higher poration efficiency and post-poration viability than that with unipolar square pulses [16]. Still, to date most electroporation setups continue to use unipolar square pulses of unspecified or uncontrolled rise and fall times. The pulses are applied on the cell through a dispersive connection, which can generate harmonics and distort the waveform actually experienced by a cell. Empirically, we found harmonics as high as 10 MHz to be still effective in electroporation [10]. To elucidate the fundamental dynamics in pulsed electroporation, we resorted to a four-step procedure to evaluate the waveform experienced by a cell [17]: 1) Characterize the propagation property of the electrical connection at each harmonic frequency. 2) Decompose an applied pulse into its harmonic components in the frequency domain. 3) Evaluate each harmonic wave after propagating through the connection. 4) Reconstitute the harmonic waves at the cell location back into a pulse in the time domain. To avoid such a complicated procedure, the present single-cell electroporation setup is based on a single-frequency CW signal applied to a linear and ultrawideband CPW from 9 kHz to 9 GHz, so waveform distortion is not of great concern. It is hoped that by analyzing the poration and healing dynamics at each harmonic frequency, it can help elucidate the combined effect by a square pulse.

For the present single-cell electroporation setup, instead of relying on certain estimated average field, we found it necessary to numerically evaluate the electric field by finite-element electromagnetic simulation [10]. Considering that the electrode spacing is typically comparable to the cell size, the electric field distribution can be highly nonuniform and greatly disturbed by the presence of a cell. The detailed analysis of electric field with the cell in the electrode spacing allows comparison of threshold voltages with other electroporation setups. This approach is also important because: 1) We resuspend the cell in an ion-free medium, so that the field mostly goes through the cell to create hot spots on the membrane. 2) Although the length of the electrical transmission line is much shorter than the electromagnetic wavelength, its propagation characteristics along the line must still be considered, especially when its amplitude is doubled as it is

0018-9294 (c) 2018 IEEE. Personal use is permitted, but republication/redistribution requires IEEE permission. See http://www.ieee.org/publications_standards/publications/rights/index.html for more information.

This article has been accepted for publication in a future issue of this journal, but has not been fully edited. Content may change prior to final publication. Citation information: DOI 10.1109/TBME.2018.2885781, IEEE Transactions on Biomedical Engineering

reflected from the electrode spacing where a cell is trapped. 3) The tapered electrodes help focus the field locally and its magnitude is sensitive to the radius of the electrode curvature, as well as the exact position of the cell within the electrode spacing. Furthermore, different from most other single-cell electroporation setups, we use DEP instead of mechanical means to trap a cell, which allows a cell to be quickly trapped and detrapped, so that the small signal due to the presence of a cell can be extracted from a drifting background and the same trap can be used repeatedly [11].

Unique to this study is that the microwave transmission coefficient was observed to scatter more significantly even below the poration threshold of 1.5 V. We ruled out the instrumentation factor because Fig. 5(b) shows that the transmission coefficient did not scatter significantly when measured with 100-kHz, 0–2.5-V signals and *without* a cell trapped. Recall that as far as the instrument is concerned, the CPW gap is essentially an open circuit, whether a cell is trapped there or not. Thus, the elevated scatter under the sub-threshold voltage is not caused by the direct coupling of the instrument, but perhaps due to an unknown cell compartment that allows the poration and microwave signals to couple nonlinearly. To our knowledge, this is the first time pre-poration electrical cell response is recorded. The mechanism behind such fluctuation requires further study and is beyond the scope of this paper.

Presently, after a Jurkat cell was porated, its microwave transmission coefficient would take approximately 100 s to recover (Fig. 6 and Fig. 7), which is comparable with the recovery time reported in the literature. For example, after a HeLa cell was electroporated, its PI intensity and RF impedance would recover in approximately 200 s [18], [19]. As mentioned in the introduction, it is difficult to compare the poration threshold of one single-cell setup with another, without knowing the detailed field distribution in each case. However, so long as a cell is porated to the same extent as characterized by PI dye for instance, it should heal similarly after poration. This underscores the usefulness of the transmission coefficient not only for poration, but also healing.

To prove that the present DEP signal had little effect on the cell vitality during the few seconds it took to trap it, another experiment was conducted with the 5-MHz, 2.2-V DEP signal applied on a Jurkat cell up to 2.5 h after it was already trapped. It can be seen from Fig. 9 that the red fluorescence intensity increases by less than 5% only after 1.5 h, whereas the green fluorescence decreases by less than 40% after 2 h. In particular, the green intensity remains constant during the first half hour. Thereafter it decreases slowly perhaps by photobleaching. Finally, based on another experiment involving a much stronger microwave signal and a temperature-sensitive dye [10], the present microwave signal at −18 dBm is unlikely to cause heating or other undesirable side effects.

V. Conclusion

For the first-time, we were able to correlate the change in the microwave transmission coefficient with the change in fluorescence intensity *during* and *after* electroporation, as well as to use the microwave transmission coefficient to distinguish

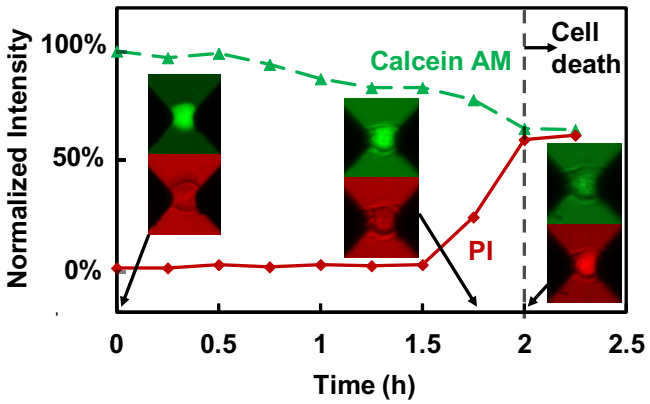

Fig. 9. Evolution of changes in red (♦) and green (▲) fluorescence intensities of a Jurkat cell under prolonged exposure to a DEP signal of 5 MHz and 2.2 V without any intentional electroporation signal. Insets correspond to red and green fluorescence images taken at 0, 1.75, and 2 h of DEP exposure.

reversible electroporation from *irreversible* electroporation. As the result, we quantified 1.5–2.0 V as the voltage range for reversible poration of a Jurkat cell by a 100 kHz CW signal in the present setup. Although it is difficult to compare the present threshold field with that of other single-cell electroporation setups, the present voltage range appears to be reasonable. For example, it is consistent with the fact that at 100 kHz most of the voltage drops across the cell membrane at opposite poles, and the generally accepted transmembrane potential required for electroporation is on the order of 1 V.

The present setup uses a poration signal with an amplitude on the order of 1 V to extend the poration time to the order of 10 s. At 100 kHz, this voltage drops almost entirely across the cell membrane for efficient poration [10]. The low voltage and long poration time also allow the cell morphology, poration, vitality, and electrical properties to be monitored in real time simultaneously *during* poration. Having demonstrated that, the poration voltage can be increased and the poration time shortened, so that the result can be more effectively compared with that in the literature. The present video camera is capable of 100 frame/s, whereas the microwave network analyzer can perform a single-frequency measurement in 1 ms. It will be relatively straightforward to shorten the poration time to less than 1 s without missing detailed dynamics. If the poration time is shortened further to the millisecond range, then the cell can only be monitored before and after (not during) poration as often done in the literature.

Present microwave characterization is performed at 9 GHz, a frequency known to be most sensitive to cytoplasm properties instead of membrane properties [20]. Having established the utility of the microwave transmission coefficient at 9 GHz, we can expand the measurement to include a lower frequency that is known to be sensitive to the membrane properties. In addition to the transmission coefficient, the microwave reflection coefficient may be utilized. In fact, we have characterized both the transmission and reflection coefficients of a Jurkat cell from 9 kHz to 9 GHz, and analyzed their sensitivity at different frequencies to membrane resistance, membrane capacitance, cytoplasm resistance, cytoplasm capacitance, etc. [20] The analysis can be used to guide future experiments.

0018-9294 (c) 2018 IEEE. Personal use is permitted, but republication/redistribution requires IEEE permission. See http://www.ieee.org/publications_standards/publications/rights/index.html for more information.

This article has been accepted for publication in a future issue of this journal, but has not been fully edited. Content may change prior to final publication. Citation information: DOI 10.1109/TBME.2018.2885781, IEEE Transactions on Biomedical Engineering

Whereas so far only the poration of Jurkat cells has been characterized, the same microwave characterization setup has been used to monitor the viability of various mammalian cells [11] and *E. coli* bacteria [21]. In the future, it will be interesting to use the same setup to correlate the microwave transmission coefficient with poration of other cell types and to make this technique generally applicable. If successful, single-cell transfection experiments can be conducted on many different types of cells efficiently without the interference of fluorescent dyes. This way, microwave characterization can bring about new insight into the mechanism for ions and molecules to permeate through a cell membrane.

The main purpose of this work is to correlate the microwave transmission coefficient with electroporation of a cell. For convenience, we followed previous protocols to resuspend the cell in an ion-free medium [11]. Although less efficient, others have performed electroporation with cells in a physiological medium. Recently, we have succeeded in using the same experimental setup to characterize *E. coli* in their culture medium [21]. In the future, we should be able to repeat the same correlation study with a cell in its culture medium.

REFERENCES

[1] D. Miklavcic, *Handbook of Electroporation*. New York, NY, USA: Springer, 2016. [Online]. Available:https://link.springer.com/referencework/10.1007%2F978-3-319-26779-1?page=1#toc.

[2] S. Le Gac and I. van Uitert, “Electroporation in microfluidic devices,” *ibid*, pp. 1–20.

[3] T. Batista Napotnik, “Fluorescent indicators of membrane permeabilization due to electroporation,” *ibid*, pp. 1–19.

[4] S. Šatkauskas *et al*., “Different cell viability assays following electroporation in vitro,” *ibid*, pp. 1–14.

[5] S. Romeo *et al*., “Water influx and cell swelling after nanosecond electropermeabilization,” *Biochim. Biophys. Acta.,* vol. 1828, no. 8, pp. 1715–1722, Mar. 2013.

[6] O. Français and B. Le Pioufle, “Single cell electrical characterization techniques,” in [1], pp. 1–18.

[7] Q. Castellví, B. Mercadal, and A. Ivorra, “Assessment of electroporation by electrical impedance methods,” in [1], pp. 1–18.

[8] A. Tamra *et al.,* "Microwave monitoring of single cell monocytes subjected to electroporation," *IEEE Trans. Microw. Theory Techn.,* vol. 65, no. 9, pp. 3512–3518, Sep. 2017.

[9] H. Li *et al.*, "Correlation between morphology change and microwave property during single-cell electroporation," in *IEEE MTT-S Int. Microwave Symp. (IMS) Dig.*, Honolulu, HI, USA, Jun. 2017, pp. 1–4.

[10] H. Li *et al.,* "Distributed effect in high-frequency electroporation of biological cells," *IEEE Trans. Microw. Theory Techn.,* vol. 65, no. 9, pp. 3503–3511, Sep. 2017.

[11] Y. Ning *el al.*, “Broadband electrical detection of individual biological cells,” *IEEE Trans. Microw. Theory Techn.,* vol. 62, no. 9, pp. 1905−1911, Sep. 2014.

[12] W. Longsine-Parker *et al.*, "Microfluidic electro-sonoporation: A multi-modal cell poration methodology through simultaneous application of electric field and ultrasonic wave," *Lab Chip,* vol. 13, no. 11, pp. 2144–2152, Jun. 2013.

[13] H. Y. Wang and C. Lu, “Electroporation of mammalian cells in a microfluidic channel with geometric variation,” *Anal. Chem.,* vol. 78, no. 14, pp. 5158–5164, Jun. 2006.

[14] D. C. Chang, “Cell poration and cell fusion using an oscillating electric field,” *Biophys. J.*, vol. 56, no. 4, pp. 641–652, Oct. 1989.

[15] D. C. Chang, P. Q. Gao, and B. L. Maxwell, “High efficiency gene transfection by electroporation using a radio-frequency electric field,” *Biochim. Biophys. Acta,* vol. 1092, no. 2, pp. 153–160, Apr. 1991.

[16] E. Tekle, R. D. Astumian, and P. B. Chock, “Electroporation by using bipolar oscillating electric field: An improved method for DNA transfection of NIH 3T3 cells,” *Proc. Natl. Acad. Sci. U. S. A.,* vol. 88, no. 10, pp. 4230–4234, May. 1991.

[17] A. Denzi *et al*., “Assessment of cytoplasm conductivity by nanosecond pulsed electric fields,” *IEEE Trans. Biomed. Eng.,* vol. 62, no. 6, pp. 1595−1603, Jun. 2015.

[18] S. C. Chen *et al.*, "Delivery of molecules into cells using localized single cell electroporation on ITO micro-electrode based transparent chip," *Biomed. Microdevices,* vol. 14, no. 5, pp. 811–817, Oct. 2012.

[19] X. Guo and R. Zhu, "Controllable in-situ cell electroporation with cell positioning and impedance monitoring using micro electrode array," *Sci Rep.,* vol. 6, pp. 31392, Aug. 2016.

[20] X. Ma *et al.*, “Ultra-wideband impedance spectroscopy of a live biological cell,” *IEEE Trans. Microw. Theory Techn.,* vol. 66, no. 2, pp. 1099−1107, Feb. 2018.

[21] H. Li et al., “Differentiation of live and heat-killed *E. coli* by microwave impedance spectroscopy,” *Sens. Actuators B,* vol. 255, no. 2, pp. 1614–1622, Feb. 2018.

0018-9294 (c) 2018 IEEE. Personal use is permitted, but republication/redistribution requires IEEE permission. See http://www.ieee.org/publications_standards/publications/rights/index.html for more information.